

Geologic Sweet Spot Identifier: A Machine Learning Approach to Optimal Drilling Locations

Aditya Holla, Ameera Aslam, Beshoy Shaker, Elijah Flores, Jayant Bhaskarun

CONTENTS

1.0 ABSTRACT.....	4
2.0 EXECUTIVE SUMMARY.....	5
3.0 INTRODUCTION.....	6
3.1 CONTEXT.....	6
3.2 PROBLEM	7
3.3 RESPONSE.....	7
4.0 BACKGROUND	8
4.1 PRIOR RESEARCH IN SWEET SPOT IDENTIFICATION	8
4.2 MACHINE LEARNING APPLICATIONS IN RESERVOIR CHARACTERIZATION	9
5.0 METHODS.....	9
5.1 DATA COLLECTION	10
5.2 DATA CLEANING AND MUNGING.....	10
<i>5.2.1 Missing and Zero Values.....</i>	<i>10</i>
<i>5.2.2 Outlier Detection and Transformation</i>	<i>10</i>
<i>5.2.3 Feature Selection and Redundancy Control.....</i>	<i>11</i>
5.3 FEATURE ENGINEERING.....	11
<i>5.3.1 Variable Renaming and Encoding.....</i>	<i>11</i>
<i>5.3.2 Correlation and Multicollinearity Handling</i>	<i>11</i>
<i>5.3.3 Normalization</i>	<i>12</i>
<i>5.3.4 Exploratory Statistical Analysis</i>	<i>12</i>
5.4 ANALYSIS METHODS.....	12
<i>5.4.1 Regression Modeling and Validation</i>	<i>12</i>
<i>5.4.2 Sweet Spot and Quality Index Formulation</i>	<i>13</i>
5.5 ALGORITHMS.....	13

5.6 SPATIAL MODELING AND VISUALIZATION	13
6.0 RESULTS	14
6.1 SWEET SPOT SCORE DISTRIBUTION	14
6.2 INTERPOLATED MAP OF RESERVOIR PRODUCTIVITY	15
7.0 DISCUSSION/INTERPOLATION	15
7.1 GEOLOGICAL IMPLICATION OF HIGH-SCORE ZONES	15
7.2 RESERVOIR CONNECTIVITY AND ANISOTROPY	16
7.3 COMPARTMENTALIZATION AND FLOW BARRIERS.....	16
7.4 MODEL LIMITATIONS AND SOURCES OF UNCERTAINTY	17
7.5 SUPPORT FOR THE STUDY HYPOTHESIS	17
7.6 UNEXPECTED RESULTS AND THEIR INTERPRETATION.....	17
7.7 UNEXPECTED RESULTS AND THEIR INTERPRETATION.....	18
7.8 IMPLICATIONS FOR FIELD DEVELOPMENT AND DECISION-MAKING.....	18
8.0 CONCLUSION	19
9.0 REFERENCED	20
10.0 FIGURE CAPTIONS	22

1 1.0 ABSTRACT

2 Identifying optimal drilling locations (“sweet spots”) remains one of the most critical and
3 uncertain challenges in oil and gas field development. Traditional approaches rely heavily on
4 geological interpretation and seismic analysis, which, while valuable, are often subjective and
5 difficult to scale across large spatial domains. Recent advances in data analytics and machine
6 learning provide an opportunity to augment these traditional methods with objective, data-
7 driven decision frameworks. This study addresses the problem of sweet-spot identification
8 using a well-level dataset provided by ConocoPhillips, consisting of 55 wells and 14
9 petrophysical, production, and spatial variables.

10

11 Building on prior work in spatial reservoir characterization and machine-learning-based
12 production forecasting, this project integrates exploratory data analysis, spatial interpolation,
13 feature engineering, and non-linear predictive modeling. Missing data were handled using
14 median imputation, and extreme water-production outliers were isolated to prevent bias in
15 productivity measures. Spatial kriging was applied to visualize reservoir and production trends
16 while explicitly accounting for interpolation uncertainty. A composite Quality Index was
17 developed using the harmonic mean to generate a conservative, balanced ranking of wells
18 based on porosity, permeability, pressure, and production metrics. Facies quality was modeled
19 using Random Forest classification, while XGBoost was selected for sweet-spot prediction due
20 to its ability to capture non-linear interactions and variable dependencies within the dataset.

21

22 The resulting Sweet Spot Prediction Map reveals spatial zones of elevated production potential
23 and highlights pressure and rock quality as the dominant controls on productivity. Using peak-
24 detection with spatial separation constraints, six high-confidence, non-overlapping drilling
25 targets were identified. These results align with previous studies emphasizing the importance
26 of integrated geological and data-driven workflows, while demonstrating the added value of
27 uncertainty-aware spatial modeling.

28

29 Overall, this study demonstrates that combining spatial analytics, composite reservoir indices,
30 and machine learning provides a robust, interpretable, and scalable framework for drilling
31 optimization. The methodology offers practical implications for reducing exploration risk,
32 improving capital allocation, and supporting data-informed decision-making in modern
33 reservoir development.

34 **2.0 EXECUTIVE SUMMARY**

35 1. What is the problem?

36 Selecting optimal drilling locations in oil and gas fields is inherently uncertain and
37 capital-intensive. Traditional decision-making relies heavily on geological interpretation
38 and isolated production metrics, which can be subjective and difficult to scale spatially.
39 This creates a risk of drilling in sub-optimal zones, increasing development costs and
40 reducing recovery efficiency. ConocoPhillips sought a data-driven, spatially integrated
41 workflow to improve confidence in sweet-spot identification using existing well data.

42 2. What was your approach?

- 43 • We developed an integrated geology–machine learning–spatial analytics workflow
44 using well-level petrophysical, production, and spatial data. Our process included:
- 45 • Cleaning and exploring the raw well data to understand spatial and production
46 behavior.
- 47 • Applying spatial kriging to visualize reservoir trends with uncertainty awareness.
- 48 • Constructing a composite Quality Index using the harmonic mean to create a
49 balanced well-performance ranking.
- 50 • Modeling facies quality with Random Forest.
- 51 • Using XGBoost to capture non-linear relationships and generate a Sweet Spot
52 Prediction surface.
- 53 • Applying peak-detection algorithms to identify high-confidence drilling targets while
54 enforcing spatial separation.

55 3. What did you learn?

- 56 • Pressure and rock quality (porosity and permeability) are the strongest drivers of well
57 productivity.

- 58 • Porosity and permeability are largely redundant with facies, confirming the
59 importance of geological context.
60 • Machine learning improves consistency in ranking wells but must be constrained by
61 physical geology.
62 • Spatial uncertainty increases near field boundaries, emphasizing the need for risk-
63 aware interpretation.
64 • Sweet-spot patterns form consistent spatial clusters rather than isolated single-point
65 highs.

66 4. What are your recommendations?

- 67 • Prioritize drilling in high-pressure, high-rock-quality zones identified by the Sweet
68 Spot Map.
69 • Focus on the six highest-confidence drilling locations identified through peak-
70 detection.
71 • Avoid over-reliance on kriging without raw well control—always interpret with
72 observed data.
73 • Use the Quality Index for relative ranking, not absolute production forecasting.
74 • Expand well density in low-confidence areas to improve future spatial accuracy.
75 • Incorporate depletion-corrected pressure in future modeling to improve long-term
76 reliability.

77 **3.0 INTRODUCTION**

78 **3.1 Context**

79 Oil and gas exploration plays a critical role in meeting global energy demands, yet it remains one
80 of the most uncertain and capital-intensive stages of field development. Drilling decisions are
81 traditionally guided by geological interpretation, seismic data, and expert judgment. While these
82 methods provide valuable subsurface insight, they rely on large volumes of complex,
83 heterogeneous data and often require subjective integration across multiple disciplines. As
84 reservoirs become more heterogeneous and development costs rise, the industry increasingly
85 requires objective, scalable, and data-driven tools to support drilling decisions.

86 Recent advances in data science and machine learning have enabled more systematic analysis of
87 geological, petrophysical, and production data. Prior studies show that reservoir properties such
88 as porosity, permeability, depth, facies, and pressure are strong indicators of well productivity,
89 and that machine learning models can outperform traditional statistical approaches in predicting
90 production behavior (Ibrahim et al., 2022; Du et al., 2024). More recently, machine learning has
91 also been applied directly to spatial sweet spot identification, demonstrating its potential to
92 predict high-productivity zones using integrated reservoir and completion data (Machine
93 Learning Sweet Spot Identification..., 2023). These advances highlight the growing role of
94 analytics in modern reservoir evaluation and field development.

95 ***3.2 Problem***

96 Despite progress in predictive modeling, most existing studies focus primarily on well-level
97 production prediction rather than direct spatial identification of optimal drilling locations.
98 Traditional sweet spot identification often depends on isolated geological indicators or seismic
99 attributes without fully integrating geological quality, production behavior, spatial variability,
100 and model uncertainty into a unified framework. Additionally, subsurface data commonly exhibit
101 strong variable correlation, spatial sparsity, pressure depletion effects, and extreme production
102 outliers, all of which challenge reliable modeling and interpretation. As a result, there remains a
103 critical need for a transparent, interpretable, and spatially explicit workflow that links machine
104 learning predictions to physical reservoir controls in order to support high-confidence drilling
105 decisions.

106 ***3.3 Response***

107 This study addresses this gap by developing an integrated, data-driven sweet spot identification
108 workflow using a well-level dataset provided by ConocoPhillips, consisting of 55 wells and 14
109 petrophysical, production, and spatial variables. The workflow combines exploratory data
110 analysis, feature engineering, machine learning, and spatial visualization to quantify reservoir
111 quality and drilling potential. A composite Quality Index based on the harmonic mean was
112 developed to provide a conservative, balanced representation of reservoir performance.
113 Ensemble machine learning models were applied to capture non-linear geological–production

114 relationships and generate a Sweet Spot Prediction Score. Spatial kriging was then used as a
115 visualization tool to interpolate model outputs across the field while preserving actual well
116 control and uncertainty awareness.

117 The resulting framework directly translates raw well data into actionable drilling guidance while
118 maintaining physical interpretability and risk awareness. This approach supports data-informed
119 drilling decisions, reduces the reliance on subjective interpretation, and contributes to the
120 growing application of machine learning in reservoir characterization and field development
121 planning.

122 **4.0 BACKGROUND**

123 ***4.1 Prior Research in Sweet Spot Identification***

124 Previous research in petroleum engineering has extensively examined the geological and
125 petrophysical factors that control hydrocarbon productivity. Rock properties such as porosity,
126 permeability, facies, and total depth are widely recognized as key indicators of reservoir quality
127 and fluid flow potential. Early efforts to identify productive zones relied primarily on statistical
128 regression and petrophysical interpretation; however, these traditional approaches were often
129 limited by subsurface heterogeneity and complex nonlinear relationships.

130 Ibrahim et al. (2022) demonstrated that predictive modeling can effectively capture production
131 behavior across diverse formations using long-term regression analysis of oil, gas, and water
132 outputs. Similarly, Du et al. (2024) applied deep learning techniques to forecast oil production in
133 U.S. reservoirs, achieving improved predictive performance compared to conventional empirical
134 models. While these studies provided valuable insight into production behavior at existing wells,
135 they primarily focused on forecasting outputs rather than identifying new drilling locations.

136 More recent studies have begun shifting toward integrating petrophysical and spatial parameters
137 to locate areas of enhanced reservoir potential, commonly referred to as “sweet spots.” However,
138 many existing models still evaluate wells individually and do not fully incorporate coordinate-
139 based spatial relationships that reveal geographic clusters of productivity. This limitation reduces

140 their usefulness for field-scale exploration planning. The present study builds upon this prior
141 work by integrating geological, production, and spatial features into a unified framework for
142 mapping zones of high production potential.

143 ***4.2 Machine Learning Applications in Reservoir Characterization***

144 Machine learning has become an increasingly important tool in reservoir characterization due to
145 its ability to model nonlinear relationships and process large, multidimensional datasets.
146 Techniques such as regression, random forests, and neural networks have been widely used to
147 predict production trends, estimate reservoir properties, and automate geologic interpretation.
148 These methods often outperform traditional statistical techniques, particularly when data are
149 incomplete or noisy.

150 Lavi et al. (2024) introduced data-driven imputation strategies to address missing production
151 data, demonstrating that machine learning can preserve data integrity while improving predictive
152 accuracy. Li et al. (2024) developed a weighted productivity framework incorporating
153 permeability, porosity, and depth, establishing permeability and porosity as dominant controls on
154 reservoir performance. Their hierarchy of control factors provides a foundation for the multi-
155 variable scoring approach adopted in this study.

156 Recent advances increasingly combine machine learning with spatial analysis, allowing models
157 to move beyond isolated well prediction toward field-scale reservoir visualization. By integrating
158 spatial coordinates with petrophysical and production variables, predictive models can identify
159 geographic trends in productivity. This study advances this direction by applying machine
160 learning to quantify relationships among key variables and visualizing these patterns through a
161 three-dimensional Sweet Spot Map.

162 **5.0 METHODS**

163 This section describes the data sources, preprocessing steps, feature engineering procedures,
164 analytical methods, machine learning algorithms, and spatial interpolation techniques used to
165 identify high-potential drilling locations. All analyses are conducted in Python to ensure full
166 reproducibility.

167 **5.1 Data Collection**

168 The dataset is provided by ConocoPhillips and consists of measurements from 55 wells. The
169 variables include petrophysical properties (porosity, permeability in x and y directions, facies,
170 and total measured depth), production metrics (oil production, gas production, water production,
171 and reservoir pressure), and spatial information (bottom-hole x and y coordinates). These data
172 form the basis for all subsequent statistical, machine learning, and geospatial analyses.

173 **5.2 Data Cleaning and Munging**

174 **5.2.1 Missing and Zero Values**

175 The dataset is first inspected to identify missing and zero values. Five wells (Wells 8, 9, 27, 28,
176 and 47) contain zero entries in oil and gas production columns. Prior to imputation, summary
177 statistics and distribution plots (including boxplots) are generated for all production variables to
178 verify that zero values reflect valid operational conditions rather than data-entry errors. These
179 visual diagnostics reveal strong skewness and outlier sensitivity, motivating the use of median-
180 based imputation.

181 Following Lavi et al. (2024), missing or zero entries are treated as operational artifacts such as
182 temporary well shutdowns or sensor errors rather than random omissions. Median imputation is
183 applied because it is robust to extreme values and preserves the empirical distribution of the data
184 while maintaining the small sample size.

185 **5.2.2 Outlier Detection and Transformation**

186 Outliers are detected using the interquartile range (IQR) method. Water production displays
187 strong positive skewness with several extreme values. To stabilize variance while preserving
188 geological meaning, a MinMax scaling was applied to all numerical variables.

189 Outlier behavior is also assessed separately within each facies group to identify facies-specific
190 anomalies in both production and petrophysical variables. Facies-stratified boxplots are

191 generated to determine whether transformations should be applied uniformly across the dataset
192 or selectively by geological classification, ensuring consistent scaling across all rock types.

193 **5.2.3 Feature Selection and Redundancy Control**

194 Non-predictive identifiers such as well name and well number are removed. The future pressure
195 prediction variable is excluded to prevent data leakage. Statistical hypothesis testing is used to
196 evaluate feature significance; variables with limited predictive power, such as future_pressure,
197 were evaluated for removal when appropriate.

198 To capture total energy output rather than treating oil and gas separately, a “Predicted
199 Production” metric was created by combining normalized oil and gas production. This composite
200 variable represents unified energy production and accounts for wells that are predominantly oil-
201 or gas-driven. The metric is used as an alternative exploratory target variable to evaluate unified
202 productivity behavior during preliminary modeling.

203 **5.3 Feature Engineering**

204 **5.3.1 Variable Renaming and Encoding**

205 All variables are standardized using snake-case naming conventions to ensure computational
206 consistency. The categorical facies variable is one-hot encoded into binary features for
207 integration into regression and machine learning models.

208 **5.3.2 Correlation and Multicollinearity Handling**

209 Pearson correlation analysis identifies strong dependencies between permeability and porosity,
210 and between depth and pressure, indicating potential multicollinearity. To mitigate instability
211 caused by correlated predictors, quality scores were created as a way of testing data with more
212 than one variable in a single metric.

213 **5.3.3 Normalization**

214 Continuous variables are normalized using min–max scaling to the [0,1] interval:

215

$$X_{norm} = \frac{X - X_{min}}{X_{max} - X_{min}}$$

216 This ensures all parameters contribute proportionally regardless of native measurement units.

217 Categorical and dimensionless parameters remain in encoded format for interpretability.

218 **5.3.4 Exploratory Statistical Analysis**

219 As part of the exploratory workflow, descriptive statistics and boxplots are generated for all key
220 variables including porosity, permeability, oil, gas, and water production. Wells are grouped by
221 facies and facies-stratified production plots are constructed for oil, gas, water, and derived ratios.
222 These procedures document geological variability patterns prior to modeling and support later
223 physical interpretation of machine learning outputs.

224 **5.4 Analysis Methods**

225 **5.4.1 Regression Modeling and Validation**

226 Rather than focusing on linear regression as our initial thought process entailed, we modeled
227 production using an XGBoost regressor trained on spatial coordinates, depth, porosity,
228 harmonic-mean permeability, past pressure, and an engineered facies-quality index. This allows
229 the model to capture threshold effects and interactions which linear regressions can't explain or
230 show.

231 We also used Kriging to interpolate depth and other continuous properties onto a regular grid.
232 The XGBoost-based Sweet Spot Score was then evaluated on this grid and combined with kriged
233 fields to generate continuous maps, on which spatial clustering, anisotropy, and connectivity

234 were interpreted. Minimum-distance filters relative to existing wells and peak-finding algorithms
235 were also applied to identify candidate infill locations.

236 **5.4.2 Sweet Spot and Quality Index Formulation**

237 An initial composite Sweetspot Score is explored using XGBoost feature importance weightings.
238 It ends up prioritizing pressure and depth as dominant controls. The final Sweetspot Score is a
239 combination of pressure, depth, permeability, and porosity to create a variable for the synthetic
240 wells created called “Predicted Production.” To further isolate geological quality from production
241 noise, a Quality Index (QI) is constructed using harmonic aggregation of porosity, permeability,
242 pressure, and GOR. A Facies Quality Score (FQS) is also computed to isolate lithologic
243 influence independent of depth and production. These indices serve as inputs to subsequent
244 spatial prediction.

245 **5.5 Algorithms**

- 246 • Random Forest Regressor for feature importance and exploratory imputation
247 • Ordinary Kriging for spatial interpolation
248 • XGBoost (final model) for Sweet Spot prediction

249 XGBoost is selected due to its ability to capture nonlinear feature interactions, robustness to
250 correlated predictors, and superior performance under small-sample conditions.

251 **5.6 Spatial Modeling and Visualization**

252 The Sweetspot Scores are visualized using bottom-hole coordinates (`bh_x`, `bh_y`) and total depth.
253 To transform discrete well measurements into continuous fields, Ordinary Kriging is applied
254 using the PyKrig library.

255 Kriging estimates values at unsampled locations using weighted averages of known points while
256 modeling spatial autocorrelation through a variogram. A spherical variogram model is
257 automatically fit using least-squares optimization. A 150×150 spatial grid is defined across the

258 field bounds, and kriging is applied independently to permeability, porosity, depth, pressure, and
259 Sweetspot Score.

260 KNN interpolation was evaluated as a computational benchmark but was rejected due to its lack
261 of uncertainty quantification and poor spatial continuity. Kriging remains the primary
262 interpolation method due to its optimal statistical properties and uncertainty estimation.

263 Sweet Spot surfaces were visualized using the Kriging mapping package with depth contours
264 overlaid. These maps reveal spatial clustering of high-scoring wells and allow identification of
265 prospective drilling targets between existing wells based on the warmth of the color shown.

266 Prediction uncertainty is largest near field boundaries outside the convex hull of wells and lowest
267 near dense well clusters.

268 **6.0 RESULTS**

269 ***6.1 Sweet Spot Score Distribution***

270 An interpolation of the Sweetspot Score was created to visualize the spatial variation of
271 reservoir productivity across the study area (Figure 13). The Sweetspot Score, calculated as a
272 weighted linear combination of permeability, porosity, production, and depth parameters,
273 provides a unified measure of reservoir quality and flow potential. The imputed weighting
274 scheme was calculated from the XGBoost model, which identifies pressure and depth as
275 dominant controls on well oil and gas output.

276 The resulting Sweetspot Score distribution differentiates high- and low-productivity wells
277 across the dataset. Higher scores generally occur within intermediate depth intervals and regions
278 exhibiting stronger permeability and porosity values. In contrast, lower scores are concentrated
279 in deeper or low-permeability zones where compaction and diagenesis likely reduce pore
280 connectivity.

281 Overall, the Sweetspot Score successfully integrates petrophysical and production variables
282 into a single interpretable metric that reflects the underlying physical properties governing
283 hydrocarbon flow.

284 ***6.2 Interpolated Map of Reservoir Productivity***

285 The Kriging Sweetspot Map (Figure 13) combines borehole spatial coordinates (`bh_x`, `bh_y`)
286 with total measured depth to visualize the Sweetspot Score as a color mapped surface. Linear
287 interpolation converts discrete well data into a continuous surface, revealing both lateral and
288 vertical continuity in reservoir productivity potential.

289 Warmer colors (orange to red) represent higher Sweetspot Scores and indicate zones where
290 permeability and porosity combine with favorable production metrics, suggesting enhanced
291 hydrocarbon flow potential. Cooler colors (yellow) correspond to lower-quality zones with
292 reduced pressure, depth, permeability, or porosity.

293 Several high-score clusters are visible, laterally connected at intermediate depths. These areas
294 likely correspond to depositional or structural features such as channel sands or high
295 permeability stratigraphic units that promote greater fluid connectivity. Shallower and mid-depth
296 regions consistently exhibit stronger scores than deeper sections, where compactional effects
297 and diagenetic cementation may diminish permeability.

298 The resulting visualization highlights spatially coherent regions of high reservoir potential
299 and provides a foundation for interpreting geological trends that control productivity.

300 **7.0 DISCUSSION/INTERPOLATION**

301 ***7.1 Geological Implication of High-Score Zones***

302 The Sweet Spot Score, built from the XGBoost production model and the facies-probability–
303 based facies quality index, highlights coherent high-score clusters that coincide with wells in
304 higher-porosity, higher-permeability facies. These zones are concentrated in structurally

305 lower areas where kriged depth, facies quality, and historical production all agree,
306 suggesting thicker, less compacted reservoir intervals with better preserved pore networks.
307 Laterally continuous high-score trends follow the mapped facies architecture rather than
308 appearing as isolated artifacts, which is consistent with channel-like or sheet-sand bodies
309 that maintain reservoir quality across multiple locations. This behavior indicates that the
310 Sweet Spot Score is capturing integrated rock and fluid-flow behavior rather than simply
311 mirroring a single input variable.

312 ***7.2 Reservoir Connectivity and Anisotropy***

313 Since the score uses harmonic-mean permeability (perm_{hm}) and a facies classifier trained on
314 perm_x , perm_y , porosity, depth, and pressure, the sweet-spot map more clearly expresses
315 directional permeability trends. Elongated high-score corridors align with the dominant
316 permeability direction inferred from $\text{perm}_x/\text{perm}_y$ and from the facies map, implying preferential
317 flow pathways along depositional fabrics or paleoflow directions. These anisotropic corridors
318 link multiple high-quality wells and coincide with smoother pressure gradients in the XGBoost
319 predictions, supporting an interpretation of laterally connected flow units rather than isolated
320 “good” wells.

321 ***7.3 Compartmentalization and Flow Barriers***

322 Where high Sweet Spot Scores terminate abruptly against low-score regions, the updated maps
323 often coincide with facies transitions, rapid depth changes, or low-quality facies identified by the
324 facies-quality model. These boundaries are interpreted as potential intra-reservoir baffles or
325 compartments (shaly intervals, tight facies, or stratigraphic pinch-out) that limit lateral pressure
326 communication. In contrast, areas where high-score clusters remain contiguous across several
327 grid cells and wells are likely to represent more continuous reservoir bodies with better
328 connectivity. The combination of raw-data facies maps, kriged depth contours, and the
329 sweet-spot surface makes it easier to distinguish structural versus stratigraphic controls on
330 connectivity and to identify where additional wells would most efficiently connect to existing
331 high-quality flow units.

332 ***7.4 Model Limitations and Sources of Uncertainty***

333 Despite the methodological improvements such as explicit facies-quality modeling, separation of
334 training and validation data, and clearer feature engineering, the workflow remains constrained
335 by the limited dataset (55 wells) and the strong correlations among key predictors (facies,
336 porosity, permeability, and pressure). The XGBoost feature-importance and facies-model
337 analyses show that rock-quality and pressure effects are intertwined; as a result, statements about
338 “dominant” drivers must be interpreted as predictive, not strictly causal. Spatial interpolation via
339 kriging still introduces uncertainty away from well control, especially near the model edges
340 where the sweet-spot surface is extrapolated. In addition, water production and some pressure
341 behaviors remain noisy and occasionally counterintuitive, indicating that more targeted EDA and
342 perhaps separate water-handling models would be beneficial. Despite these constraints, the
343 overall workflow demonstrates that even small datasets can yield physically interpretable
344 insights when combined with transparent modeling and sound geological reasoning.

345 ***7.5 Support for the Study Hypothesis***

346 The central hypothesis of this study is that integrating geological, petrophysical, production, and
347 spatial features within a unified machine-learning and geostatistical framework can improve the
348 identification of high-potential drilling zones. The results support this hypothesis. High Sweet
349 Spot Scores consistently align with wells located in high-porosity, high-permeability facies and
350 with zones of stronger historical production. The spatial clustering of predicted sweet spots
351 further confirms that the model is capturing coherent geological patterns rather than random
352 production variability. These outcomes demonstrate that the integrated workflow successfully
353 translates multi-source data into a physically interpretable prediction of reservoir potential.

354 ***7.6 Unexpected Results and Their Interpretation***

355 Several unexpected behaviors were observed during analysis. In some areas, elevated Sweet Spot
356 Scores occurred where historical oil production was moderate rather than extreme. This behavior

357 is attributed to the model's emphasis on balanced reservoir quality through the harmonic mean–
358 based Quality Index, which penalizes single-parameter dominance. Additionally, localized high
359 water production occasionally overlapped high permeability zones, reducing Sweet Spot Scores
360 in regions that might otherwise appear attractive based solely on rock quality. These outcomes
361 highlight the importance of incorporating multiple production indicators and demonstrate that
362 high permeability alone does not guarantee favorable oil productivity.

363 **7.7 Unexpected Results and Their Interpretation**

364 Consistent with prior studies by Ibrahim et al. (2022), Du et al. (2024), and Li et al. (2024), this
365 project confirms that permeability and porosity remain the dominant controls on reservoir
366 productivity. However, unlike earlier studies that primarily focused on well-level prediction, this
367 work advances the literature by extending machine-learning predictions into a spatially
368 continuous sweet spot map using ordinary kriging. While previous studies emphasized
369 production forecasting, the present framework explicitly targets **geographic drilling**
370 **optimization**, bridging a key gap between predictive modeling and practical field development
371 planning.

372 **7.8 Implications for Field Development and Decision-Making**

373 The spatial Sweet Spot framework developed in this study provides a practical tool for guiding
374 drilling decisions in data-limited reservoirs. By ranking potential drilling zones based on
375 integrated rock quality, pressure behavior, and production indicators, the approach supports more
376 efficient well placement and reduces the risk associated with exploratory drilling. The
377 methodology is directly transferable to other fields with limited well control and can be extended
378 to include seismic attributes, time-dependent production, and geomechanical constraints.
379 Ultimately, this workflow demonstrates how data-driven modeling can complement traditional
380 geological interpretation to improve reservoir management and capital allocation.

381 **8.0 CONCLUSION**

382 This study develops an integrated geologic–machine learning workflow to identify production-
383 driven sweet spots by combining spatial interpolation, facies analysis, and gradient-boosted
384 prediction. The central hypothesis of this work is that sweet spots can be reliably identified using
385 a unified framework that integrates rock quality, pressure, and spatial context rather than relying
386 on production alone. The results support this hypothesis.

387 Kriging maps of oil, gas, water, porosity, permeability, pressure, gas–oil ratio, facies, facies
388 quality, and the final Sweet Spot Score reveal a structurally coherent reservoir in which
389 production highs systematically track structural position and associated rock-quality trends rather
390 than appearing as isolated anomalies. Facies-conditioned boxplots demonstrate that Facies 1 and
391 2 consistently exhibit the highest porosity and permeability, confirming their role as the primary
392 reservoir facies and establishing a physical foundation for the engineered machine-learning
393 features.

394 By explicitly addressing the strong correlation between facies, porosity, and permeability, the
395 workflow uses a facies quality score and a harmonic-mean-based quality index to compress
396 redundant petrophysical information into stable, outlier-robust predictors. After this correction,
397 XGBoost feature importance and kriged production surfaces show that pressure and depth,
398 modulated by rock quality, emerge as the dominant predictive controls on the Sweet Spot
399 surface, while extreme water producers are deliberately excluded to prevent optimization bias.
400 Facies-specific uncertainty analysis further reveals elevated classification risk within Facies 3,
401 identifying zones where additional geological control is needed before development decisions.

402 The final Sweet Spot Map, combined with peak local maxima detection and spatial spacing
403 constraints, yields six spatially independent drilling candidates located within the structurally
404 aligned “sweet-spot ring.” These candidates represent relative, not absolute, production forecasts,
405 but they are supported by mutually consistent trends across pressure, facies, petrophysical
406 properties, and historical production, providing a defensible basis for ranked drilling decisions
407 within the convex hull of existing wells.

408 Overall, this work demonstrates that when kriging-based spatial context, facies-aware feature
409 engineering, and nonlinear machine-learning models such as XGBoost are carefully constrained
410 by geology, artificial intelligence can move beyond black-box prediction to deliver interpretable,
411 uncertainty-aware sweet-spot recommendations for field development planning.

412 Future work should include:

- 413 1. Expanding the dataset with additional wells or time-lapse production to improve
414 generalization and uncertainty control.
415 2. Integrating seismic or log-derived attributes to strengthen spatial and stratigraphic
416 resolution.

417 **9.0 REFERENCED**

418 **1. Du, J., Zheng, J., Liang, Y., & Shahzad, K. 2024.**
419 A deep learning-based approach for predicting oil production: A case study in the United
420 States. *Energy* 288: 129688.
421 <https://doi.org/10.1016/j.energy.2023.129688>

422 **2. Ibrahim, N. M., Alharbi, A. A., Alzahrani, T. A., Abdulkarim, A. M., Alessa, I. A.,
423 Hameed, A. M., Albabtain, A. S., Alqahtani, D. A., Alsawwaf, M. K., & Almuqhim,
424 A. A. 2022.**
425 Well-performance classification and prediction: Deep learning and machine-learning
426 long-term regression experiments on oil, gas, and water production. *Sensors* 22(14):
427 5326.
428 <https://doi.org/10.3390/s22145326>

429 **3. Li, J., Chen, Z., & Zhang, M. 2024.** “Quantitative Evaluation of Main Control
430 Factors Affecting Well Productivity in Tight Sandstone Reservoirs.” *Processes*, 12(9):
431 1890. <https://doi.org/10.3390/pr12091890>

432 **4. Lavi, B., Bertini Jr., J.R., Pires, L.C.O., and Schiozer, D.J. 2024.**
433 Handling Missing Data on Short-term Oil Rate Forecasting in a Pre-salt Offshore Field
434 Benchmark. *ROG.e 2024: Technical Paper*, 1–11.
435 <https://doi.org/10.48072/2525-7579.roge.2024.3726>

436 **5. Leem, J., & Chen, H. 2023.**
437 Machine Learning Sweet Spot Identification and Performance Validation Utilising
438 Reservoir and Completion Data from Unconventional Reservoir in British Columbia,
439 Canada. *SPE-215220-MS*.
440 <https://www.researchgate.net/publication/374503924>

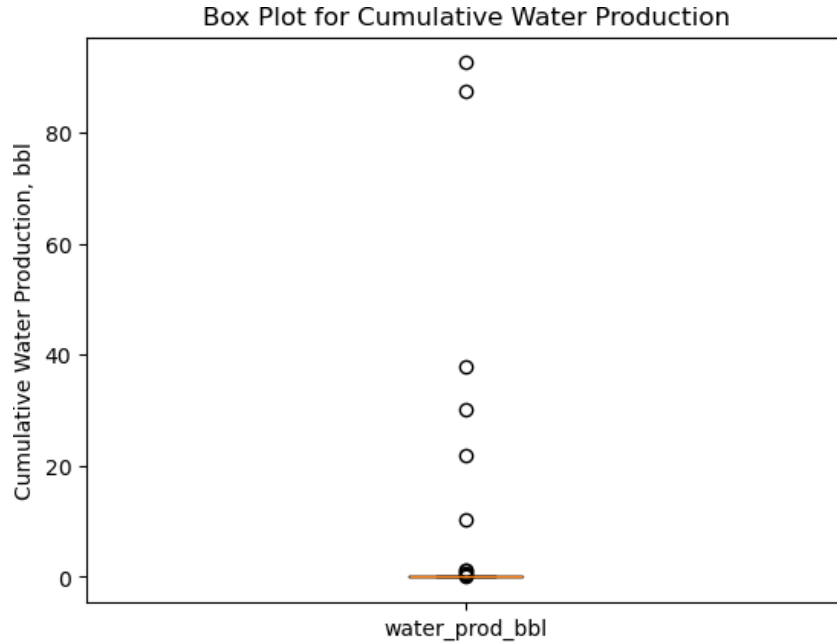
441 **6. Meyer, R., and Krause, F. F. 2006.**
442 Permeability anisotropy and heterogeneity of a sandstone reservoir analogue: An

443 estuarine to shoreface depositional system in the Virgelle Member, Milk River
444 Formation, Writing-on-Stone Provincial Park, Southern Alberta. *Bulletin of Canadian*
445 *Petroleum Geology* 54(4): 301–318.
446 <https://doi.org/10.2113/gscpgbull.54.4.301>

447 **7. ScienceDirect Topics. 2025.**
448 Reservoir Compartmentalization—An Overview. *Earth and Planetary Sciences*.
449 [https://www.sciencedirect.com/topics/earth-and-planetary-sciences/reservoir-](https://www.sciencedirect.com/topics/earth-and-planetary-sciences/reservoir-compartmentalization)
450 [compartmentalization](https://www.sciencedirect.com/topics/earth-and-planetary-sciences/reservoir-compartmentalization)

451 **10.0 FIGURE CAPTIONS**

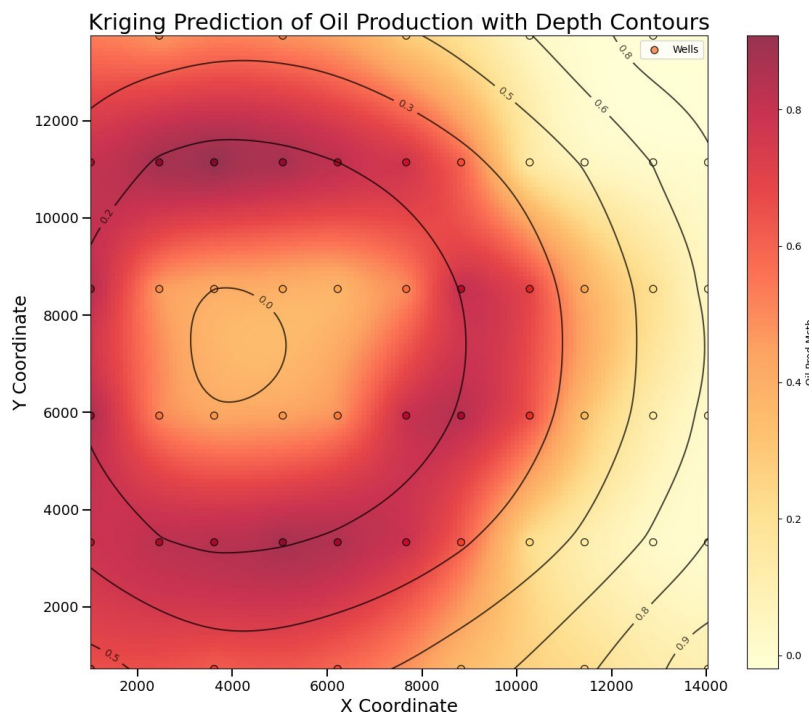
449



450

451 Figure 1: Box Plot for Water Production

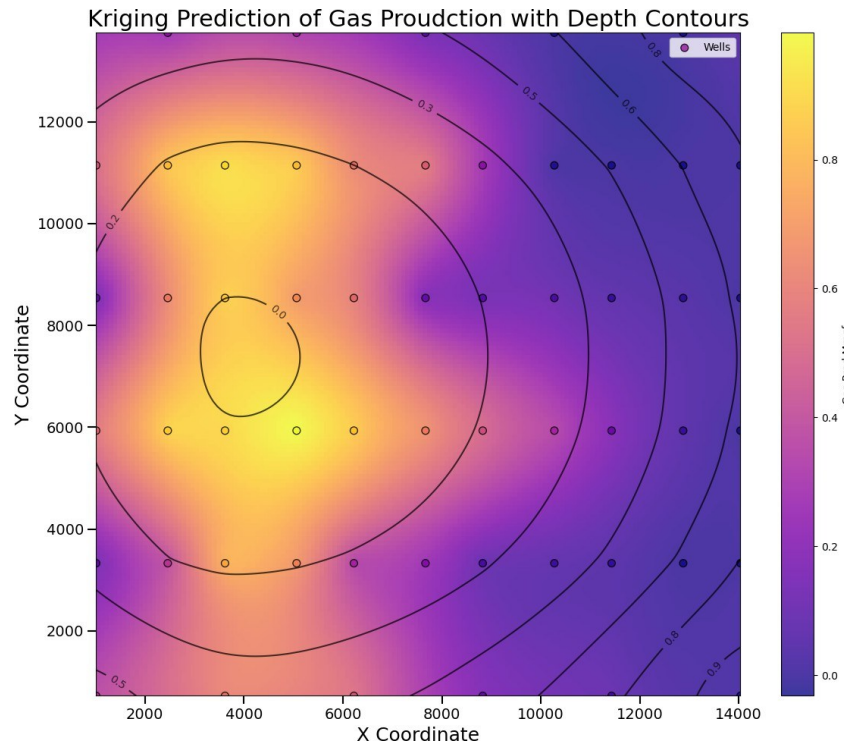
452



453

454 Figure 2: Kriging Map of Oil Production

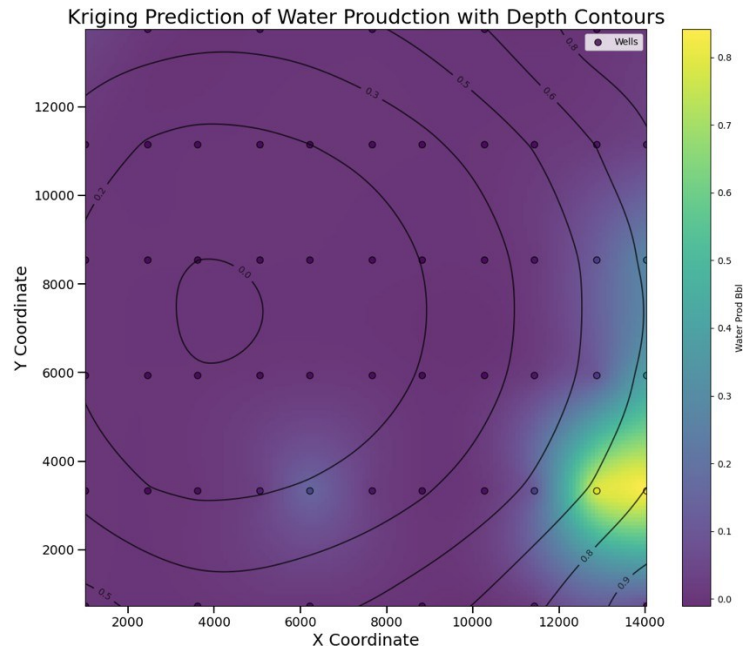
455



456

457 Figure 3:Kriging Map of Gas Production

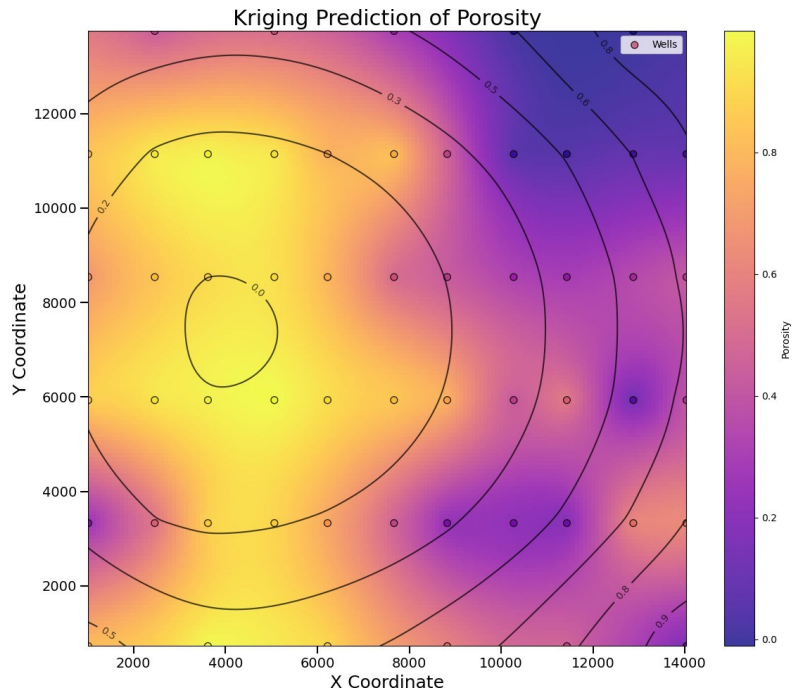
458



459

460 Figure 4: Kriging Map of Water Production

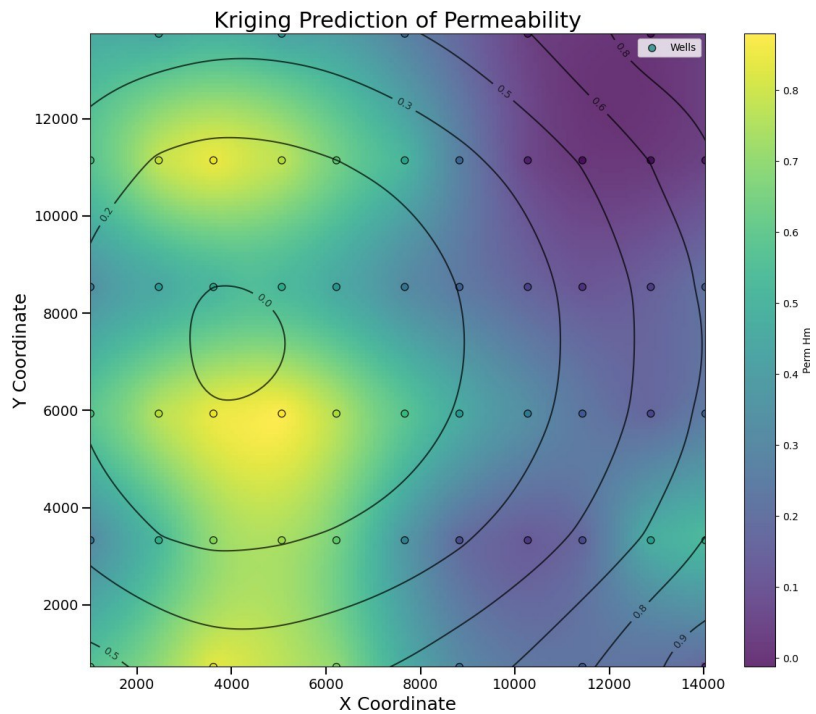
461



462

463 Figure 5: Kriging Map of Porosity

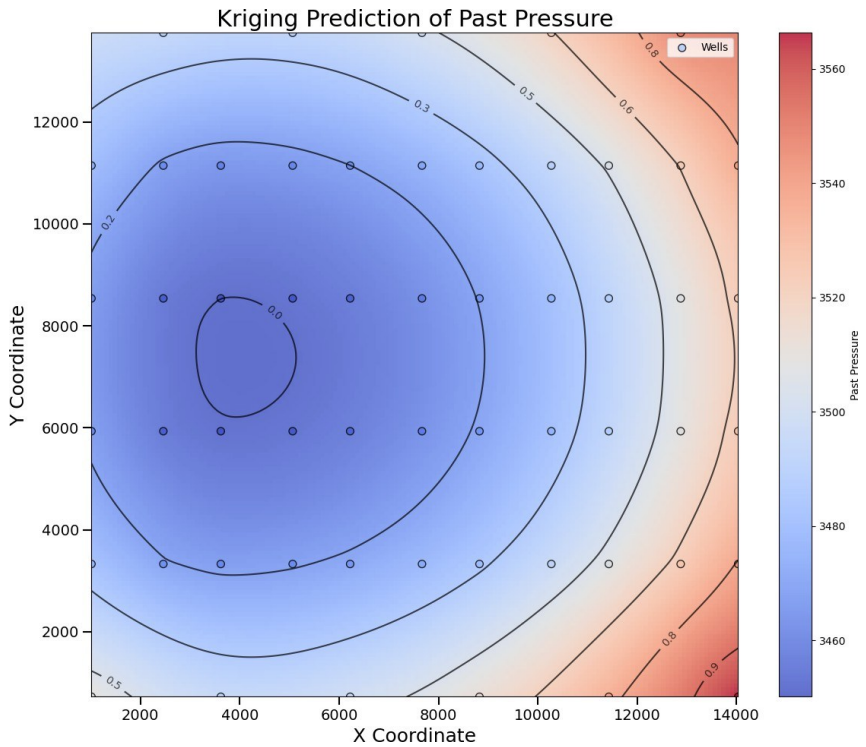
464



465

466 Figure 6: Kriging Map of Permeability

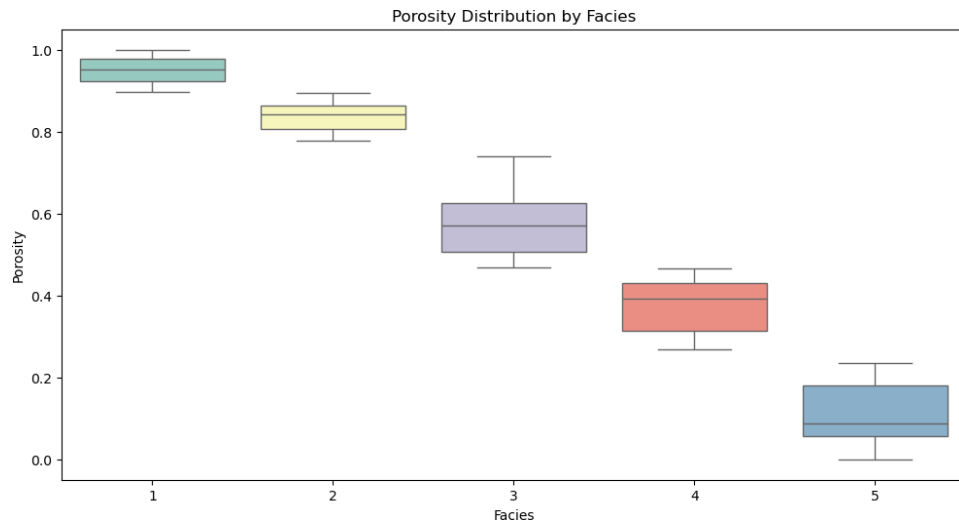
467



468

469 Figure 7: Kriging Map of Pressure

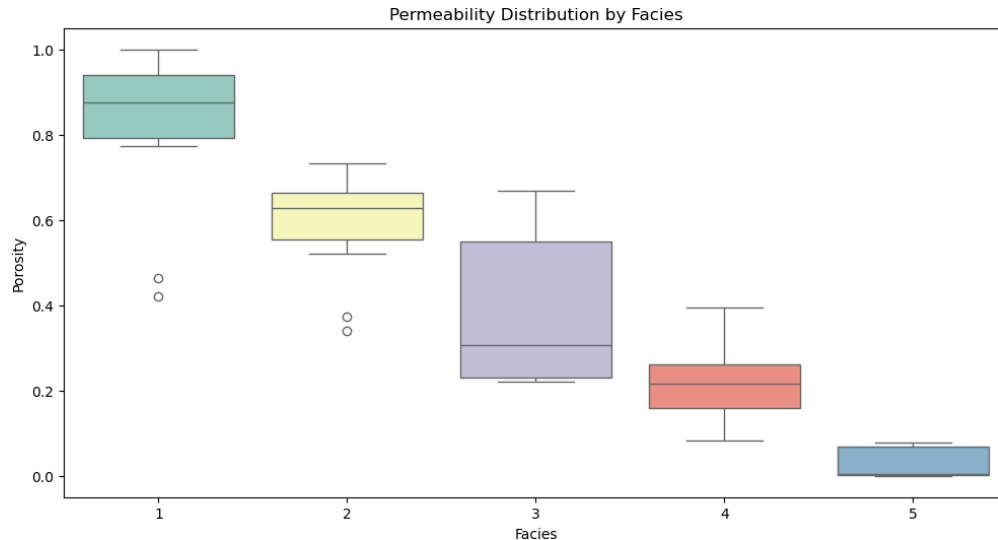
470



471

472 Figure 8: Porosity Distribution by Facies

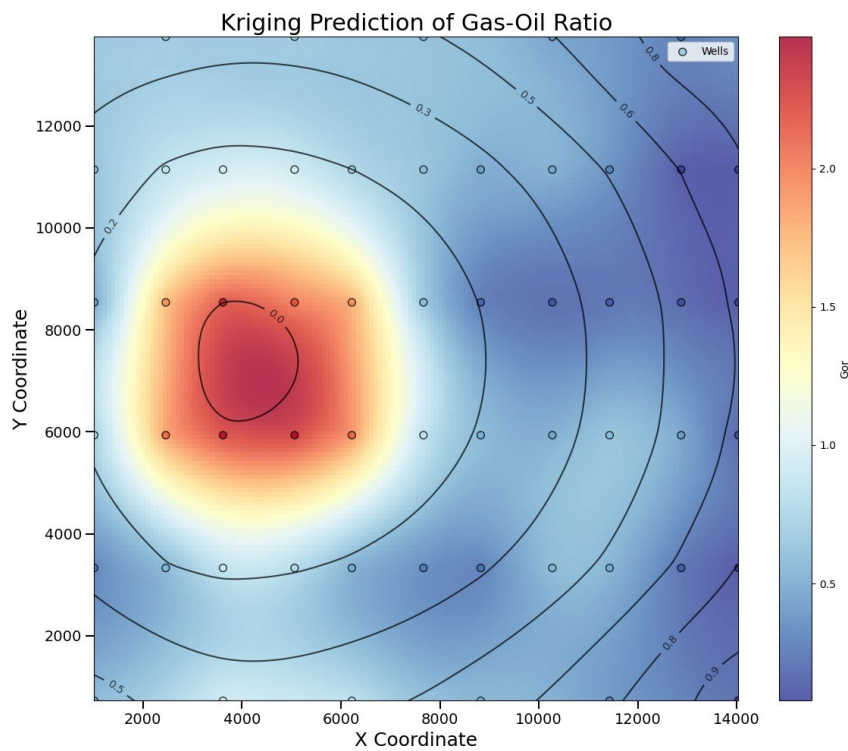
473



474

475 Figure 9: Permeability Distribution by Facies

476

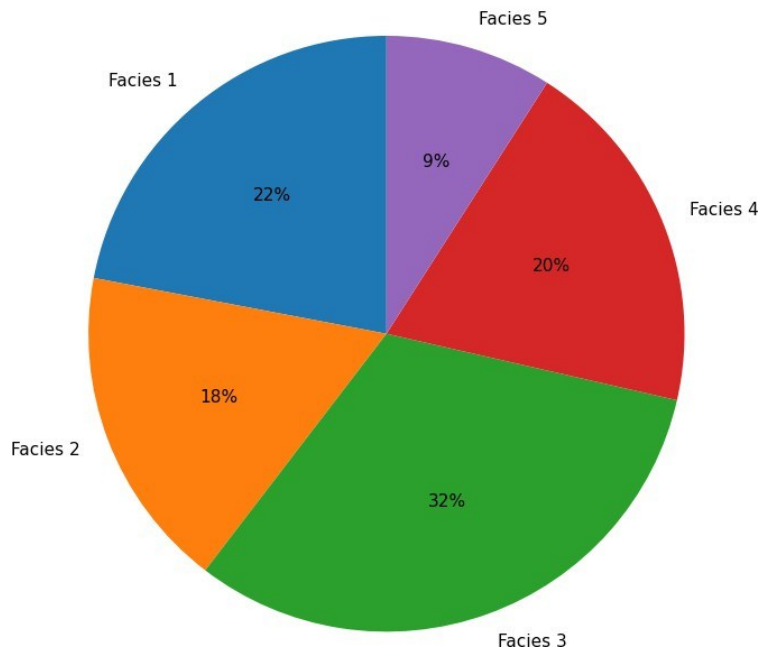


477

478 Figure 10: Kriging Map of Gas-Oil Ratio

479

Relative Uncertainty by Facies Type

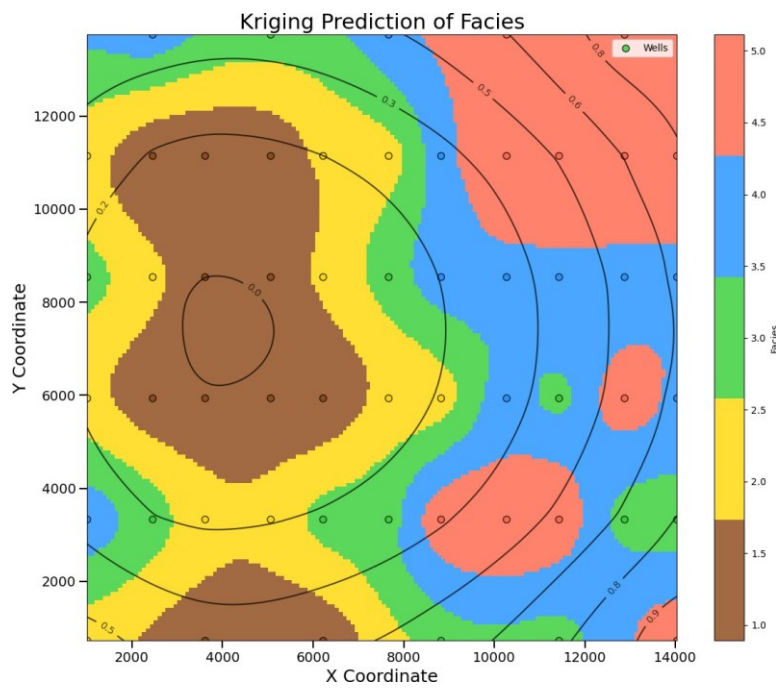


480

481 Figure 11: Relative Uncertainty by Facies (Random
482 Forest)

483

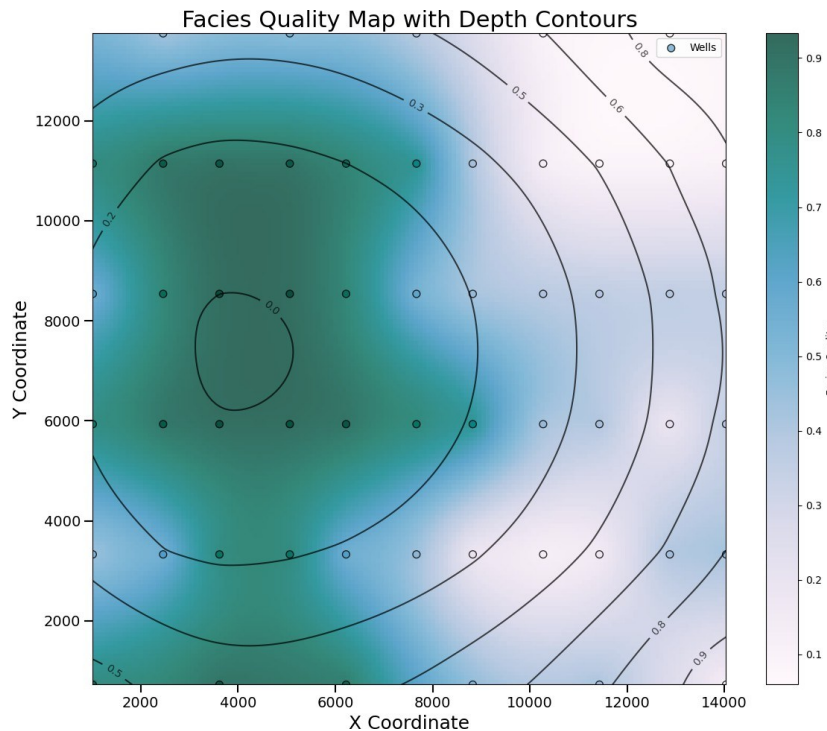
484



485

486 Figure 12: Kriging Map of Facies Distribution

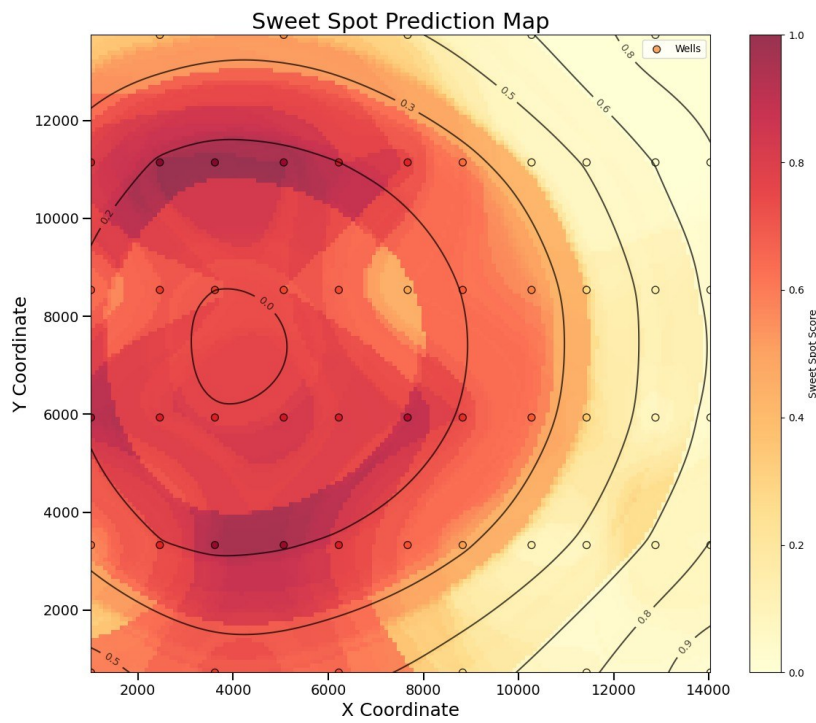
487



488

489 Figure 13: Kriging Map of Facies Quality Score

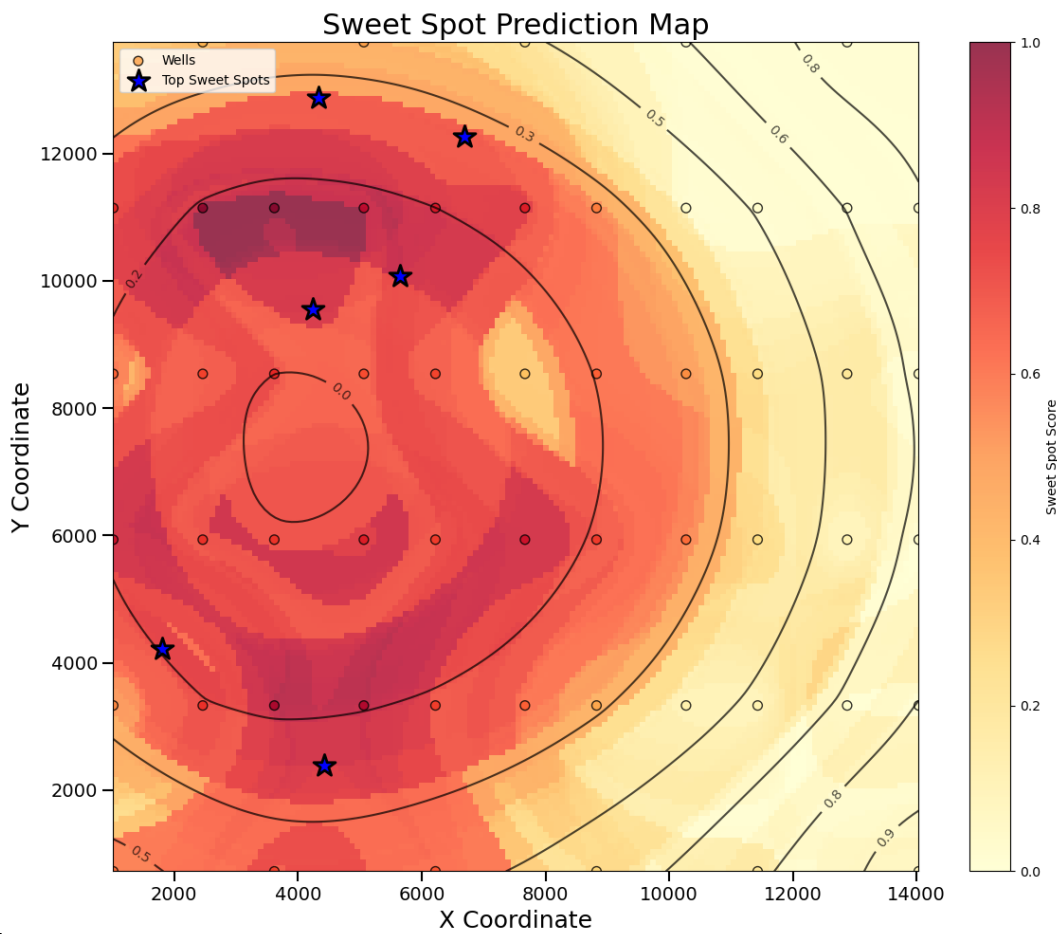
490



491

492 Figure 14: Kriging Map of Sweetspot Scores

493



494

495 Figure 15: Kriging Map of Sweetspot Scores overlaid with the six highest scores